Rbpj deletion in hepatic progenitor cells attenuates endothelial responses in a mouse model of cholestatic liver disease

Sanghoon Lee[1], Lu Ren[1], Aditi Paranjpe[2], Ping Zhou[1], Andrew Potter[3], Stacey S. Huppert[4,5], Soona Shin[1,6]

[1]Division of Pediatric General and Thoracic Surgery, Cincinnati Children's Hospital Medical Center, Cincinnati, Ohio, USA
[2]Department of Information Services, Cincinnati Children's Hospital Medical Center, Cincinnati, Ohio, USA
[3]Cardiology Clinic, Cincinnati Children's Hospital Medical Center, Cincinnati, Ohio, USA
[4]Division of Gastroenterology, Hepatology & Nutrition, Cincinnati Children's Hospital Medical Center, Cincinnati, Ohio, USA
[5]Department of Pediatrics, University of Cincinnati College of Medicine, Cincinnati, Ohio, USA
[6]Department of Surgery, University of Cincinnati College of Medicine, Cincinnati, Ohio, USA

Author Contributions: Sanghoon Lee and Soona Shin conceptualized the work, designed experiments, interpreted the data, and wrote the initial draft. Sanghoon Lee, Lu Ren, and Ping Zhou performed experiments. Stacey S. Huppert and Andrew Potter contributed to the optimization of experiments and design of the study. Sanghoon Lee, Lu Ren, and Aditi Paranjpe contributed to data acquisition, analysis, and visualization. All authors contributed to reviewing and editing the manuscript.

Correspondence: Soona Shin, Division of Pediatric General and Thoracic Surgery, Cincinnati Children's Hospital Medical Center, Cincinnati, Ohio 45229, USA. E-mail: soona.shin@cchmc.org

Financial support and sponsorship: This work was supported by the National Cancer Institute of the National Institutes of Health (NIH) R37CA225807 to S.S.; and the NIH

Public Health Service Grant P30DK078392 (Integrative Morphology Core and Gene Analysis Core of the Digestive Diseases Research Core Center in Cincinnati).

Conflict of interest: Nothing to report.

Keywords: Hepatic progenitor cells; endothelial cells; ductular reaction; liver disease; Rbpj

Abbreviations: αSMA, alpha smooth muscle actin; ALP, alkaline phosphatase; ALT, alanine aminotransferase; AST, aspartate aminotransferase; CK19, cytokeratin 19; CKO, conditional knockout; DDC, 3,5-diethoxycarbonyl-1,4-dihydrocollidine; FDR, false discovery rate; Foxl1, forkhead box L1; GFAP, glial fibrillary acidic protein; GSEA, gene set enrichment analysis; HNF4α, hepatocyte nuclear factor 4 alpha; HPC, hepatic progenitor cell; HSC, hepatic stellate cell; LSEC, liver sinusoidal endothelial cell; NK, natural killer; OPN, osteopontin; pDC, plasmacytoid dendritic cell; qPCR, quantitative polymerase chain reaction; RBPJ, recombination signal binding protein for immunoglobulin kappa J region; sNuc-seq, single-nucleus RNA sequencing; UMAP, uniform manifold approximation and projection; VEGFA, vascular endothelial growth factor A; WT, wild-type; YFP, yellow fluorescent protein.

Data availability: Raw data for single-nucleus RNA sequencing are in the process of being deposited in Gene Expression Omnibus (accession number to be added upon acceptance).

ABSTRACT

Background and Aims: Since the role of hepatic progenitor cells (HPCs) constituting ductular reactions in pathogenesis remains ambiguous, we aimed to establish the in vivo cause-and-effect relationship between HPCs and angiogenesis, a process associated with chronic liver disease progression. We previously demonstrated that peritumoral ductules are associated with angiogenesis in liver tumors and forkhead box L1 (Foxl1)-expressing murine HPCs secrete angiogenic factors in vitro. Therefore, we hypothesized that HPCs are capable of remodeling the vascular microenvironment and this function of HPCs is dependent on recombination signal binding protein for immunoglobulin kappa J region (RBPJ), a key effector of the Notch signaling pathway.

Approach and Results: We generated HPC-specific *Rbpj* conditional knockout mice using *Foxl1-Cre* and treated them with the 3,5-diethoxycarbonyl-1,4-dihydrocollidine-supplemented diet to induce cholestatic liver disease. Knockout mice displayed significant reduction of HPC proliferation and ductular reactions as well as attenuated vascular and fibrotic areas compared to control mice. Assessment of vascular endothelial growth factor A-positive areas in vivo and the effects of *Rbpj* shRNAs in vitro indicated that *Rbpj* knockout in HPCs reduces the total number of angiogenic factor-expressing cells rather than affecting angiogenic factor expression within HPCs. Single-nucleus RNA sequencing analysis indicated that conditional *Rbpj* knockout in HPCs induces transcriptional changes in endothelial cells and alters expression of genes involved in various functions of the endothelium.

Conclusion: Our findings indicate that HPCs regulate endothelial responses to cholestatic liver disease and *Rbpj* deletion in HPCs attenuates these responses, identifying novel targets for modulating angiogenesis during disease progression.

INTRODUCTION

Hepatic progenitor cells (HPCs) are facultative stem cells mainly derived from normal cholangiocytes activated in response to liver injury.[1] HPCs form ductular reactions and peritumoral ductules detected in a variety of chronic liver diseases and cancer.[2-6]

However, their causal role in disease progression remains to be tested. Previous studies reported that HPCs express paracrine factors involved in angiogenesis, fibrosis, and inflammation in the context of various liver diseases such as primary biliary cirrhosis and pediatric metabolic dysfunction-associated steatotic liver disease.[7, 8] We also reported that HPCs in peritumoral ductules in the livers of patients with liver cancer express angiogenic factors, and the number and proliferation of HPCs as well as the extent of angiogenic factor expression by HPCs correlate with intra- and peritumoral angiogenesis and intratumoral proliferation.[4]

Forkhead box L1 (Foxl1)-expressing HPCs and their descendants can be labeled with yellow fluorescent protein (YFP) using the *Foxl1-Cre* transgenic mouse in multiple models of liver disease[9-11] including 3,5-diethoxycarbonyl-1,4-dihydrocollidine (DDC)-induced cholestatic liver disease.[12] HPCs isolated from DDC-fed *Foxl1-Cre;Rosa*^{YFP} mice secrete a number of paracrine factors involved in angiogenesis, fibrosis, and tumorigenesis.[13] Our in vitro data also indicated that HPCs communicate with endothelial cells in a paracrine manner to stimulate endothelial proliferation, tubulogenesis, and gene expression, implying their potential roles in angiogenesis.[13] It is becoming increasingly clear that angiogenesis plays important roles in not only in tumor development but also liver fibrosis. Several studies have reported involvement of angiogenesis in pathophysiology of liver diseases such as hepatocellular carcinoma, metabolic dysfunction-associated steatotic liver disease, cholangiopathies, and alcohol-related liver disease.[14-18] Association between HPCs and angiogenesis also has been reported, but these studies were based on correlative data or global gene disruption affecting multiple cell types.[4, 7, 19] Therefore, the causal role of HPCs in altering the endothelium of diseased liver using specific modulation of HPCs remains to be tested. Therefore, the current study aims to establish the cause-and-effect relationship between HPCs and DDC-induced endothelial responses using conditional gene modulation specific for HPCs. DDC mainly induces biliary injury but also periportal hepatocytic injury, and it is a widely used model for inducing ductular reactions and simulating cholangitis and biliary fibrosis.[12, 20, 21]

It has been demonstrated that recombination signal binding protein for immunoglobulin kappa J region (RBPJ), the effector molecule of the Notch signaling pathway, is an important regulator of biliary morphogenesis.[22] However, the study used the albumin promotor as the driver, which is active in hepatocytes, biliary cells, as well as the fetal precursor hepatoblasts. Therefore, the specific requirement of RBPJ for the proliferation and function of Foxl1-expressing postnatal HPCs during pathogenic progression remains largely unclear. Therefore, we aim to address how *Rbpj* gene deletion in HPCs affects communication of HPCs with other hepatic cells, with a focus on endothelial cells. We generated a conditional knockout mouse in which *Rbpj* is specifically deleted in HPCs by crossing *Foxl1-Cre;Rosa*^{YFP} mice[9] with *Rbpj*$^{F/F}$ mice.[23] This allowed us to determine the impact of HPC modulation on the liver microenvironment and the requirement of RBPJ in this process.

MATERIALS AND METHODS

Animal Experiments

The sources of *Foxl1-Cre*, *Rosa*^{YFP}, and *Rbpj*$^{F/F}$ mice are as described previously.[23-25] *Foxl1-Cre;Rosa*^{YFP}*;Rbpj*$^{F/+}$ mice on C57BL/6J background were used for breeding to generate *Foxl1-Cre;Rosa*^{YFP}*;Rbpj*$^{F/F}$ conditional knockout mice (CKO) and *Foxl1-Cre;Rosa*^{YFP}*;Rbpj*$^{+/+}$ wild-type littermate control mice (WT). 10- to 11-week-old male mice were fed a diet supplemented with 0.1% DDC (Envigo) for 4 weeks. All procedures have been approved by the Institutional Animal Care and Use Committee at Cincinnati Children's Hospital Medical Center.

Immunofluorescence analysis

Formalin-fixed paraffin-embedded tissue sections were subjected to immunofluorescence staining and quantification as described previously.[10] Six to eight random pictures centered on the portal area were captured for each mouse. Hepatocytes were identified based on hepatocyte nuclear factor 4 alpha (HNF4α) and morphology.[10] HPCs were

defined as *Foxl1-Cre*/YFP-labeled cells within cytokeratin 19 (CK19)- or osteopontin (OPN)-positive biliary epithelial populations.[9, 10] Image J was used for cell counting and quantification of marker-positive areas.[26] The following primary antibodies were used: GFP (Aves Labs GFP-1020), RBPJ (Cosmo Bio USA SIM-2ZRBP2), CK19 (Abcam ab52625), OPN (R&D AF808), HNF4α (R&D PP-H1415-0C), Ki67 (Thermo Fisher Scientific 14-5698-82), CD31 (Abcam ab28364), CD34 (Abcam ab81289), αSMA (Abcam ab7817), GFAP (Thermo Fisher Scientific 14-9892-82), and VEGFA (Abcam ab52917). TSA Plus Cyanine 3 System (PerkinElmer NEL744001KT) was used to amplify signals generated using antibodies for RBPJ, CD31, CD34, αSMA, and GFAP.

Cell culture

A clonally expanded HPC line that we previously established from a DDC-fed mouse was used.[9] Preparation of HPC culture medium was performed as described in our previous studies.[9, 13] HPCs were treated with lentiviral vectors expressing a non-silencing control and each of the 2 different shRNAs targeting the mouse *Rbpj* gene (VectorBuilder). Cells were maintained in the culture medium containing 5 μg/mL puromycin to select transduced cells. Cells were grown to 100% confluency and harvested for subsequent analysis.

Quantitative polymerase chain reaction

RNA isolation, cDNA synthesis, and quantitative polymerase chain reaction (qPCR) were performed as described previously.[13] Primer sequences: *Rbpj*-F: AGGAGCGATTCTCAGAGCCA, *Rbpj*-R: CAGTCCCAGCAAAAAGACGG, *Cdon*-F: CAAGCCCAAGAGACCTGAGAG, *Cdon*-R: TGTCCTTCACACAGTTTGTCCC, *Notch4*-F: CAGCAGACAGACTACGGTGG, *Notch4*-R: TGCAGTGCAGTTTTTCCCCT. Primer sequences for *Cxcl3*, *Fgf18*, *Vegfa*, and the normalizing control *Tbp* are available in our previous publication.[13]

Serum biochemistry

Blood drawn from the inferior vena cava was incubated at room temperature for 30 minutes. Serum was collected by centrifugation at 2,000g for 10 minutes at 4°C and subjected to the Research Liver Panel analysis (IDEXX BioAnalytics).

Statistical analysis

Student's t-tests or analysis of variance followed by multiple comparison tests were performed where applicable to detect the significance of differences between groups (GraphPad Prism 10). A p-value of <0.05 was considered statistically significant.

Please refer to the Supplemental Materials and Methods for additional information.

RESULTS

Ductular reactions and proliferation of HPCs are significantly reduced in mutant mice

To establish the cause-and-effect relationship between HPCs and vascular responses in cholestatic liver disease, we aimed to test the hypothesis that HPC-specific disruption of the *Rbpj* gene will attenuate ductular reactions and the subsequent communication between HPCs and endothelial cells. It has been reported that systemic inhibition of Notch signaling using a pharmacologic inhibitor reduced the number of HPCs in DDC-fed mice, and *Alb-Cre*-mediated deletion of *Rbpj* in all hepatic epithelial populations impaired biliary tubulogenesis.[22, 27] However, whether conditional *Rbpj* knockout using a promoter specific for HPCs impacts ductular reactions or not remains to be determined. We previously demonstrated that Foxl1 is a specific marker for facultative HPCs derived from normal cholangiocytes activated in response to various types of liver injury.[5, 6, 9] Since Foxl1 is not detected in uninjured healthy livers and only expressed in HPCs upon injury, the *Foxl1-Cre* transgenic mouse offers a valuable way to modulate gene expression of HPCs without affecting normal cholangiocytes. Therefore, to determine the role of RBPJ

in proliferation and differentiation of HPCs, *Foxl1-Cre;Rosa*^{YFP}*;Rbpj*$^{F/F}$ (CKO) mice and *Foxl1-Cre;Rosa*^{YFP}*;Rbpj*$^{+/+}$ (WT) control mice were treated with the DDC diet for 4 weeks (Figure 1A).

We performed immunostaining analysis of liver sections and quantified the percentage of RBPJ-expressing cells within the cytokeratin 19 (CK19)-expressing biliary population, a subset of which are *Foxl1-Cre*/YFP-labeled HPCs. While the extent of RBPJ expression was not different between CK19+YFP+ HPCs and CK19+YFP- cholangiocytes in WT mice, CK19+YFP+ HPCs in CKO mice displayed a reduced percentage of RBPJ-expressing cells compared to CK19+YFP- cholangiocytes in CKO mice as well as HPCs in WT mice, confirming that RBPJ is specifically deleted in HPCs of CKO mice (Figure 1B, C). A dramatic reduction of CK19+ cell number indicative of attenuated ductular reactions was also observed in CKO mice (Figure 2, left panel). Next, we determined the effect of RBPJ deletion on the proliferation of HPCs by quantifying the number of Ki67+ cells. Indeed, the percentage of Ki67-expressing HPCs was greatly reduced in CKO mice (Figure 2, middle panel), confirming that conditional deletion of *Rbpj* is a valid strategy to inhibit the proliferation of HPCs and ductular reactions.

The total number of HPCs is reduced in CKO compared to WT when mice are devoid of YFP-expressing hepatocytes

Next, we investigated the effect of *Rbpj* knockout on the absolute number of HPCs. Surprisingly, the total number of CK19+YFP+ HPCs was not different between WT and CKO (Figure 2, right panel), despite the dramatic reduction of CK19+ cell number in CKO. To gain a better understanding of this result, we investigated the number of lineage-labeled hepatocytes (Figure 3). We previously demonstrated that the clonal cell line expanded from a single HPC isolated from the liver of DDC-fed mice can differentiate into both hepatocytes and cholangiocytes in vitro, indicating that HPCs have bipotential differentiation capability.[9] The Notch signaling pathway is a key regulator of fetal progenitor cell differentiation toward biliary fate.[28] These imply that knocking out *Rbpj*

could affect the total pool of HPCs through two mechanisms, proliferation of HPCs and conversion of HPCs into hepatocytes.

Since *Foxl1-Cre* permanently labels cells with YFP by removing the transcriptional stop element from the DNA of *Rosa*^{YFP} reporter mice,[25] HPCs as well as hepatocytes derived from HPCs should maintain the expression of YFP. While *Foxl1-Cre*/YFP-labeled hepatocytes were not detected after 2 weeks of treatment with DDC in our previous study,[9] it has been reported that prolonged injury leads to the conversion of biliary cells into hepatocytes.[29] Indeed, YFP+ hepatocytes were detected in a fraction of animals after 4 weeks of DDC treatment in both WT and CKO groups, and the number of mice in which lineage-labeled hepatocytes are detected was modestly increased in response to conditional *Rbpj* deletion in HPCs (Figure 3A, B). We then divided mice into those with and without YFP-labeled hepatocytes and noticed that the number of HPCs was decreased upon *Rbpj* deletion only in mice without YFP+ hepatocytes (Figure 3C). In addition, comparison of CKO mice with and without YFP+ hepatocytes indicated that the HPC number was lower in the latter group (Figure 3C). These results suggest that differentiation of HPCs into hepatocytes stimulates further activation of Foxl1 expression and formation of HPCs from the remaining normal cholangiocytes. Our interpretation of elevated ductular reactions in WT compared to CKO, despite no significant changes in the total HPC number (Figure 2), is that newly formed HPCs did not substantially contribute to the expansion of ductular reactions because these cells were generated at later stages of disease progression after some HPCs had differentiated into hepatocytes. In other words, our data indicate that increased proliferation of HPCs that were present from the early stages of injury leads to the increased accumulation of CK19+ cells in WT as compared to CKO. The fact that YFP+ hepatocytes are detected only in a small fraction of the mice also suggests that the presence of YFP+ hepatocytes is not a major determinant underlying the dramatic reduction of ductular reactions in CKO mice.

Alteration of the portal microenvironment is attenuated upon Rbpj deletion in HPCs

To determine the effect of conditional knockout on liver injury, we analyzed the percent body weight loss in response to 4 weeks of DDC treatment and the liver to body weight ratio. Serum biochemistry for markers of liver injury and function was also assessed. Previous studies demonstrated that the DDC diet mainly induces cholestatic injury but also periportal hepatocytic injury.[12, 21] Indeed, the serum levels of hepatocytic injury markers aspartate aminotransferase (AST) and alanine transaminase (ALT) as well as cholestatic injury marker alkaline phosphatase (ALP) were significantly increased in DDC-fed mice compared to the age-matched chow-fed control group (Figure 4). The liver weight/body weight ratio was increased in response to DDC treatment in line with data reported in the literature.[30, 31] Bilirubin levels were also increased in response to DDC treatment, although the differences were not statistical significant due to the outliers. However, none of these markers reached statistically significant differences between DDC-fed WT and DDC-fed CKO, although there were trends toward reduced percent body weight loss ($p = 0.2007$, WT-DDC versus CKO-DDC) and ALT ($p = 0.1867$, WT-DDC versus CKO-DDC), suggesting a marginal attenuation of DDC-induced injury in the CKO group. There was no notable effect of DDC treatment or genotypes on the levels of the liver function markers albumin and total protein.

Since the DDC diet predominantly affects portal areas by inducing biliary fibrosis and ductular reactions,[12, 21] we assumed that analysis of histopathological markers focusing on the local microenvironment would reveal additional insights into how HPCs are involved in disease progression. Therefore, we performed immunostaining analysis of portal areas in which HPCs are detected (Figure 5). Based on our previous study indicating that HPCs secrete paracrine factors known to promote angiogenesis and fibrosis[4, 13] and the reported association between angiogenesis and liver fibrosis,[18] the current study investigated the impact of HPC modulation on areas occupied by endothelial cells as well as myofibroblasts. The following markers were used for analysis; CD31 is a pan-endothelial marker.[32] CD34 is expressed in vascular endothelial cells but not in liver sinusoidal endothelial cells (LSECs) in healthy livers, but its expression is detected in LSECs in diseased livers. CD34 is widely used to measure the microvessel density in liver disease[33] and is also expressed by a subset of fibroblasts and fibrocytes.

[34] Alpha smooth muscle actin (αSMA) is a well-established marker of myofibroblasts. Glial fibrillary acidic protein (GFAP) is expressed in quiescent hepatic stellate cells (HSCs).[35, 36] Our data indicate that the areas positive for CD31, CD34, and αSMA were dramatically reduced in CKO compared to WT (Figure 5), suggesting that HPCs communicate with endothelial cells and myofibroblasts and affect the portal microenvironment in an RBPJ-dependent manner. The fact that the GFAP-positive area remained unaffected suggests that modulation of HPCs does not affect the total number of quiescent HSCs but rather inhibits the activation of precursor cells (HSCs or portal fibroblasts) into myofibroblasts.

While YFP+ hepatocytes were detected in 2 out of 11 WT mice, YFP+ hepatocytes were observed in 5 out of 11 CKO mice (Figure 3B), allowing us to perform further statistical analysis within this group. We divided the CKO group into those with and without YFP+ hepatocytes to determine whether the presence of YFP+ hepatocytes affects marker-positive areas. There were no differences between CKO with and without YFP+ hepatocytes in terms of marker-positive areas supporting our interpretation that the presence of YFP+ hepatocytes is not a major determinant of phenotypes detected (Supplemental Figure S1), in line with the marginal differences of serum markers between CKO and WT (Figure 4). Correlation analysis indicated that the extent of association between the number of HPCs per area and CD31-, CD34-, and αSMA-positive areas is reduced in CKO compared to WT (Figure 6), indicating that *Rbpj* knockout decouples HPCs from vascular and fibrotic responses. In summary, our data establish the causal role of HPCs in the expansion of vascular and fibrotic areas in chronic liver disease.

Vascular endothelial growth factor A-positive area is reduced in CKO

To understand the mechanism underlying reduced endothelial area in CKO mice compared to WT mice, we investigated whether knocking down *Rbpj* in HPCs affects gene expression of angiogenic factors in vitro. HPCs were treated with lentiviral vectors expressing two different anti-*Rbpj* shRNAs (shRNA-1 and shRNA-2) as well as a non-silencing control and subjected to puromycin selection. A clonally expanded HPC line

previously established from a DDC-fed mouse[9] was used to circumvent the effect of cell heterogeneity. qPCR analysis was performed for angiogenic factors confirmed to be expressed by cultured HPCs in our previous study.[13] Both shRNAs downregulated the mRNA level of *Rbpj* as well as *Cdon* and *Notch4*, which are reported to be downstream of Notch signaling and direct targets of RBPJ (Figure 7A).[37, 38] However, the expression level of angiogenic paracrine factors *Cxcl3*, *Fgf18*, and *Vegfa* remained unchanged or even increased in response to *Rbpj* knockdown.

Since treatment with anti-*Rbpj* shRNAs did not downregulate angiogenic factor expression in HPCs, the next question we asked was whether the total number of angiogenic factor-expressing cells is reduced in response to HPC modulation. Our analysis focused on vascular endothelial growth factor A (VEGFA) because it is a representative angiogenic factor and we and other groups demonstrated that HPCs express VEGFA in the context of various human diseases such as liver cancer and cholestatic liver disease.[4, 7] Osteopontin (OPN) was used as a marker of ductular cells including OPN+YFP+ HPCs and OPN+YFP- cholangiocytes. There was a substantial overlap between VEGFA-stained and OPN-stained biliary areas both in WT and CKO (Figure 7B), and VEGFA-stained area was significantly reduced in CKO compared to WT (Figure 7C). This result suggests that reduced ductular reactions in CKO contribute to the reduced VEGFA availability. In summary, our data imply that conditional deletion of *Rbpj* in HPCs leads to reduced vascular areas through inhibition of HPC proliferation and subsequent reduction of the total number of angiogenic factor-expressing ductular cells rather than inhibition of angiogenic factor expression in HPCs.

Single-nucleus RNA sequencing identified altered gene expression in the endothelial cell cluster upon conditional modulation of HPCs

Immunostaining analysis indicated that HPCs modulate the total area occupied by endothelial cells (Figure 5), but it did not provide information on their functional alterations. Therefore, we aimed to investigate how conditional deletion of *Rbpj* in HPCs affects the transcriptome of endothelial cells by performing single-nucleus RNA sequencing (sNuc-

seq) of the livers of a CKO mouse and a WT mouse treated with the DDC diet for 4 weeks. A total of 10 cell clusters were identified in both WT and CKO mice (Figure 8A). Most clusters were represented by both genotypes with similar UMAP projections except for Cluster 0, which displayed distinct projection and nuclei number between the two genotypes (Supplemental Figure S2). We identified cluster-specific markers in an unbiased manner by determining highly expressed and unique genes in one cluster versus all other clusters using Seurat (Supplemental Materials and Methods, Supplemental Table S1). Annotation of each cluster was performed by determining the overlaps between our markers and those reported by Liang and colleagues who performed comprehensive single-cell transcriptomic analysis of mouse livers (Supplemental Table S2, Figure 8B).[39] Two hepatocyte clusters were identified, Cluster 0 (Hepatocyte-1) and Cluster 3 (Hepatocyte-2). Gene set enrichment analysis (GSEA) of cluster-enriched marker genes (Supplemental Table S2) indicated that each of the hepatocyte clusters is segregated based on distinct metabolic functions (Supplemental Table S3, Figure 8B). Non-parenchymal cell populations detected include: Cluster 2 - endothelial cell, Cluster 4 - cholangiocyte, Cluster 5 - HSC, and Cluster 9 - mesothelial cell. Immune cell populations were also identified: Cluster 1 - Kupffer cell, Cluster 6 - T/natural killer (NK) cell, Cluster 7 - B cell, and Cluster 8 - plasmacytoid dendritic cell (pDC).

While analysis of differentially expressed genes between WT and CKO indicated that conditional modulation of HPCs impacts gene expression in many clusters (Supplemental Table S4), we were particularly interested in genes downregulated in endothelial cell cluster (Cluster 2) in CKO, since they can be inferred as processes promoted by wild-type HPCs in an *Rbpj*-dependent manner. Cluster 2 expressed vascular endothelial cell markers such as *Ptprb* and *Eng* as well as the LSEC marker *Stab2* (Supplemental Table S2, Figure 8B).[40] GSEA using genes downregulated in CKO compared to WT in Cluster 2 identified various gene sets including iron update, blood clotting, calnexin-calreticulin cycle, autophagy, response to oxidative stress, and immunological functions (Figure 8C, Supplemental Table S5). These biological processes are involved in not only angiogenesis, normal functions, survival, and proliferation of LSECs and vascular

endothelial cells but also vascular dysfunction and liver disease progression.[41-49] In summary, our data indicate that conditional genetic modulation of HPCs induces transcriptomic alterations in endothelial cells.

DISCUSSION

This study aimed to determine the causal role of HPCs in vascular responses upon DDC treatment and the requirement of RBPJ in this process. The use of the *Foxl1-Cre* transgenic line allowed us to specifically delete *Rbpj* in HPCs. Our approach led to a significant finding that knocking out the *Rbpj* gene in HPCs inhibits their proliferation and attenuates ductular reactions. Furthermore, conditional modulation of HPCs was sufficient to attenuate vascular expansion, endothelial gene expression, and portal fibrosis in a mouse model of cholestatic liver disease. Our findings suggest that HPCs are capable of remodeling the portal microenvironment in response to chronic liver disease and RBPJ is required for the proliferation of HPCs and their ability to crosstalk with other hepatic cells.

We performed sNuc-seq analysis to determine the impact of HPC-specific genetic modulation on endothelial cell gene expression. Our approach is limited as sNuc-seq does not provide spatial information and *Foxl1*-expressing HPCs were not captured in our sequencing data. We chose sNuc-seq instead of single-cell RNA sequencing because hepatocyte populations in the DDC model were not represented efficiently using the latter method according to a study published by Wang and colleagues.[50] The hepatocyte representation was improved in our datasets confirming the validity of our method, but Hepatocyte-1 cluster would still require experimental validation as it displays differential UMAP distribution and nuclei number between genotypes. Here, we aim to use sNuc-seq as a proof-of-principle approach to determine the impact of conditional genetic manipulation of HPCs on gene expression in endothelial cells. Analysis of each cluster at a higher resolution and experimental validation would be necessary for an accurate interpretation of the data.

Indeed, our data indicate that conditional genetic modulation of HPCs alters the transcriptome of endothelial cells. GESA of Cluster 2 genes also indicated that the expression of many genes involved in various endothelial cell function and survival is dependent on HPCs. Experiments using anti-*Rbpj* shRNAs indicated that the expression of angiogenic factors in HPCs is not regulated by RPBJ, and attenuated vascular responses in CKO mice is attributable to the reduced number of cells providing angiogenic factors. Our in vitro study was performed in the absence of exogenous Notch ligands, because ductular cells express both Notch receptors and ligands[22] and our previous microarray data indicated enriched Jag1 and Jag2 expression in HPCs.[9] However, since other hepatic cells such as myofibroblasts can also provide Notch ligands and activate HPCs,[27] we cannot rule out the possibility that addition of exogenous ligands or investigation of direct cell-to-cell contact between HPCs and other hepatic cell types may reveal additional mechanisms involved in HPC-to-recipient cell communications.

Moreover, while sNuc-seq demonstrated the multi-faceted effects of HPC modulation on endothelial gene expression, it does not tell whether this interaction results in enhanced tissue regeneration or exacerbation of liver disease, since hepatic angiogenesis is involved in both physiological regeneration and pathogenesis.[51] It is possible that *Rbpj* deletion in HPCs attenuates vascular responses by hampering overall progression of disease in a cell non-autonomous way rather than directly regulating HPCs' ability to communicate with recipient cells. Additionally, while RBPJ mediates Notch signaling when a ligand activates the pathway, it may act as a transcriptional repressor in a Notch-independent manner as well.[52] Therefore, de-repression of RBPJ may also be involved in phenotypes observed in CKO mice. Complex transcriptional changes in the endothelial cell cluster and alterations in ductular reactions, vascular areas, and myofibroblast areas triggered upon conditional HPC modulation imply that multiple mechanisms are involved in these processes. Subjects of our future studies include narrowing down the key signals and downstream molecular events involved in the HPC-microenvironment crosstalk as well as the long-term functional consequences of this interaction in terms of disease progression.

Immunostaining analysis indicated the presence of YFP-labeled hepatocytes in DDC-treated livers, and the fraction of mice with these labeled hepatocytes increased upon *Rbpj* deletion in HPCs. While this result implies that *Rbpj* deletion promotes HPC-to-hepatocyte differentiation, one cannot eliminate the possibility that hepatocytes express Foxl1 in response to injury. We used a non-inducible version of *Foxl1-Cre* for continuous deletion of *Rbpj* in newly formed HPCs and to avoid the confounding effect of tamoxifen on liver disease.[53, 54] This approach is limited by the fact that we cannot distinguish HPC-derived hepatocytes from hepatocytes ectopically expressing Foxl1, as hepatocytes would express YFP in both senarios. Using an inducible model such as *Foxl1-CreER* would not solve this issue because the expression of Foxl1 is only detected in the injured liver and not the liver of chow-fed mice,[9] preventing labeling of Foxl1-expressing cells prior to DDC treatment. Nevertheless, whether lineage-labeled hepatocytes are detected or not did not affect areas occupied by endothelial cells and myofibroblasts, suggesting that labeled hepatocytes do not play an important role in this setting. Instead, our data indicate that the increased accumulation of YFP-labeled hepatocytes led to a compensatory increase in HPCs. Assessment of other conditions such as recovery from injury or testing different liver injury models may help to determine the involvement of HPC differentiation in pathological processes or regeneration.

In conclusion, our study established the cause-and-effect relationship between HPCs and remodeling of the portal microenvironment with a focus on endothelial cells, and demonstrated that RBPJ in HPCs is a suitable target for inhibiting ductular reactions and subsequent downstream effects. This study identifies novel molecular and cellular targets for modulation of angiogenesis in chronic liver disease, with the potential for broad impact given the common occurrence of ductular reactions in many liver diseases.[3]

ACKNOWLEDGEMENTS

We thank the Single Cell Genomics Facility and the Information Services for Research at Cincinnati Children's Hospital Medical Center for sequencing and bioinformatic analysis

services. We thank Dr. Tasuku Honjo for providing the *Rbpj*$^{F/F}$ mouse model used in this study.

REFERENCES

1. Yanger K, Stanger BZ. Facultative stem cells in liver and pancreas: fact and fancy. Dev Dyn 2011;240:521-529.
2. Gouw AS, Clouston AD, Theise ND. Ductular reactions in human liver: diversity at the interface. Hepatology 2011;54:1853-1863.
3. Clerbaux LA, Manco R, Van Hul N, Bouzin C, Sciarra A, Sempoux C, et al. Invasive Ductular Reaction Operates Hepatobiliary Junctions upon Hepatocellular Injury in Rodents and Humans. Am J Pathol 2019;189:1569-1581.
4. Lee S, Zhou P, Gupta A, Shin S. Reactive Ductules Are Associated With Angiogenesis and Tumor Cell Proliferation in Pediatric Liver Cancer. Hepatol Commun 2018;2:1199-1212.
5. Shin S, Kaestner KH. The origin, biology, and therapeutic potential of facultative adult hepatic progenitor cells. Curr Top Dev Biol 2014;107:269-292.
6. Holczbauer A, Wangensteen KJ, Shin S. Cellular origins of regenerating liver and hepatocellular carcinoma. JHEP Rep 2022;4:100416.
7. Franchitto A, Onori P, Renzi A, Carpino G, Mancinelli R, Alvaro D, et al. Expression of vascular endothelial growth factors and their receptors by hepatic progenitor cells in human liver diseases. Hepatobiliary Surg Nutr 2013;2:68-77.
8. Nobili V, Carpino G, Alisi A, Franchitto A, Alpini G, De Vito R, et al. Hepatic progenitor cells activation, fibrosis, and adipokines production in pediatric nonalcoholic fatty liver disease. Hepatology 2012;56:2142-2153.
9. Shin S, Walton G, Aoki R, Brondell K, Schug J, Fox A, et al. Foxl1-Cre-marked adult hepatic progenitors have clonogenic and bilineage differentiation potential. Genes Dev 2011;25:1185-1192.
10. Shin S, Upadhyay N, Greenbaum LE, Kaestner KH. Ablation of Foxl1-Cre-labeled hepatic progenitor cells and their descendants impairs recovery of mice from liver injury. Gastroenterology 2015;148:192-202 e193.
11. Shin S, Wangensteen KJ, Teta-Bissett M, Wang YJ, Mosleh-Shirazi E, Buza EL, et al. Genetic lineage tracing analysis of the cell of origin of hepatotoxin-induced liver tumors in mice. Hepatology 2016;64:1163-1177.
12. Fickert P, Stoger U, Fuchsbichler A, Moustafa T, Marschall HU, Weiglein AH, et al. A new xenobiotic-induced mouse model of sclerosing cholangitis and biliary fibrosis. Am J Pathol 2007;171:525-536.
13. Lee S, Karns R, Shin S. Mechanism of paracrine communications between hepatic progenitor cells and endothelial cells. Cell Signal 2022;100:110458.
14. Hammoutene A, Rautou PE. Role of liver sinusoidal endothelial cells in non-alcoholic fatty liver disease. J Hepatol 2019;70:1278-1291.
15. Morse MA, Sun W, Kim R, He AR, Abada PB, Mynderse M, et al. The Role of Angiogenesis in Hepatocellular Carcinoma. Clin Cancer Res 2019;25:912-920.

16. Mariotti V, Fiorotto R, Cadamuro M, Fabris L, Strazzabosco M. New insights on the role of vascular endothelial growth factor in biliary pathophysiology. JHEP Rep 2021;3:100251.
17. Yang Y, Sangwung P, Kondo R, Jung Y, McConnell MJ, Jeong J, et al. Alcohol-induced Hsp90 acetylation is a novel driver of liver sinusoidal endothelial dysfunction and alcohol-related liver disease. J Hepatol 2021;75:377-386.
18. Lin Y, Dong MQ, Liu ZM, Xu M, Huang ZH, Liu HJ, et al. A strategy of vascular-targeted therapy for liver fibrosis. Hepatology 2022;76:660-675.
19. Coll M, Arino S, Martinez-Sanchez C, Garcia-Pras E, Gallego J, Moles A, et al. Ductular reaction promotes intrahepatic angiogenesis through Slit2-Roundabout 1 signaling. Hepatology 2022;75:353-368.
20. Tephly TR, Gibbs AH, De Matteis F. Studies on the mechanism of experimental porphyria produced by 3,5-diethoxycarbonyl-1,4-dihydrocollidine. Role of a porphyrin-like inhibitor of protohaem ferro-lyase. Biochem J 1979;180:241-244.
21. Nikam A, Patankar JV, Lackner C, Schock E, Kratky D, Zatloukal K, et al. Transition between acute and chronic hepatotoxicity in mice is associated with impaired energy metabolism and induction of mitochondrial heme oxygenase-1. PLoS One 2013;8:e66094.
22. Fiorotto R, Raizner A, Morell CM, Torsello B, Scirpo R, Fabris L, et al. Notch signaling regulates tubular morphogenesis during repair from biliary damage in mice. J Hepatol 2013;59:124-130.
23. Han H, Tanigaki K, Yamamoto N, Kuroda K, Yoshimoto M, Nakahata T, et al. Inducible gene knockout of transcription factor recombination signal binding protein-J reveals its essential role in T versus B lineage decision. Int Immunol 2002;14:637-645.
24. Sackett SD, Fulmer JT, Friedman JR, Kaestner KH. Foxl1-Cre BAC transgenic mice: a new tool for gene ablation in the gastrointestinal mesenchyme. Genesis 2007;45:518-522.
25. Srinivas S, Watanabe T, Lin CS, William CM, Tanabe Y, Jessell TM, et al. Cre reporter strains produced by targeted insertion of EYFP and ECFP into the ROSA26 locus. BMC Dev Biol 2001;1:4.
26. Schneider CA, Rasband WS, Eliceiri KW. NIH Image to ImageJ: 25 years of image analysis. Nat Methods 2012;9:671-675.
27. Boulter L, Govaere O, Bird TG, Radulescu S, Ramachandran P, Pellicoro A, et al. Macrophage-derived Wnt opposes Notch signaling to specify hepatic progenitor cell fate in chronic liver disease. Nat Med 2012;18:572-579.
28. Miyajima A, Tanaka M, Itoh T. Stem/progenitor cells in liver development, homeostasis, regeneration, and reprogramming. Cell Stem Cell 2014;14:561-574.
29. Deng X, Zhang X, Li W, Feng RX, Li L, Yi GR, et al. Chronic Liver Injury Induces Conversion of Biliary Epithelial Cells into Hepatocytes. Cell Stem Cell 2018;23:114-122 e113.
30. Hao J, Shen X, Lu K, Xu Y, Chen Y, Liu J, et al. Costunolide alleviated DDC induced ductular reaction and inflammatory response in murine model of cholestatic liver disease. J Tradit Complement Med 2023;13:345-357.
31. Byrnes K, Bailey NT, Baral K, Mercer A, Joshi S, Wahby N, et al. Impaired hepatic autophagy exacerbates hepatotoxin induced liver injury. Cell Death Discov 2023;9:71.

32. Nikolic I, Todorovic V, Petrovic A, Petrovic V, Jovic M, Vladicic J, et al. Immunohistochemical Heterogeneity of the Endothelium of Blood and Lymphatic Vessels in the Developing Human Liver and in Adulthood. Cells Tissues Organs 2017;203:243-257.
33. Zhang Q, Wu J, Bai X, Liang T. Evaluation of Intra-Tumoral Vascularization in Hepatocellular Carcinomas. Front Med (Lausanne) 2020;7:584250.
34. Nishio T, Hu R, Koyama Y, Liang S, Rosenthal SB, Yamamoto G, et al. Activated hepatic stellate cells and portal fibroblasts contribute to cholestatic liver fibrosis in MDR2 knockout mice. J Hepatol 2019;71:573-585.
35. Morini S, Carotti S, Carpino G, Franchitto A, Corradini SG, Merli M, et al. GFAP expression in the liver as an early marker of stellate cells activation. Ital J Anat Embryol 2005;110:193-207.
36. Kisseleva T. The origin of fibrogenic myofibroblasts in fibrotic liver. Hepatology 2017;65:1039-1043.
37. Carlson TR, Yan Y, Wu X, Lam MT, Tang GL, Beverly LJ, et al. Endothelial expression of constitutively active Notch4 elicits reversible arteriovenous malformations in adult mice. Proc Natl Acad Sci U S A 2005;102:9884-9889.
38. Li Y, Hibbs MA, Gard AL, Shylo NA, Yun K. Genome-wide analysis of N1ICD/RBPJ targets in vivo reveals direct transcriptional regulation of Wnt, SHH, and hippo pathway effectors by Notch1. Stem Cells 2012;30:741-752.
39. Liang Y, Kaneko K, Xin B, Lee J, Sun X, Zhang K, et al. Temporal analyses of postnatal liver development and maturation by single-cell transcriptomics. Dev Cell 2022;57:398-414 e395.
40. MacParland SA, Liu JC, Ma XZ, Innes BT, Bartczak AM, Gage BK, et al. Single cell RNA sequencing of human liver reveals distinct intrahepatic macrophage populations. Nat Commun 2018;9:4383.
41. Wang CY, Babitt JL. Liver iron sensing and body iron homeostasis. Blood 2019;133:18-29.
42. Li ZW, Wang L. The role of liver sinusoidal endothelial cells in liver remodeling after injury. Hepatobiliary Pancreat Dis Int 2023;22:22-27.
43. El-Maarri O, Jamil MA, Oldenburg J. Molecular Profiling of Liver Sinusoidal Endothelial Cells in Comparison to Hepatocytes: Reflection on Which Cell Type Should Be the Target for Gene Therapy. Hamostaseologie 2020;40:S26-S31.
44. Jiang F. Autophagy in vascular endothelial cells. Clin Exp Pharmacol Physiol 2016;43:1021-1028.
45. Mooli RGR, Mukhi D, Ramakrishnan SK. Oxidative Stress and Redox Signaling in the Pathophysiology of Liver Diseases. Compr Physiol 2022;12:3167-3192.
46. Eelen G, de Zeeuw P, Treps L, Harjes U, Wong BW, Carmeliet P. Endothelial Cell Metabolism. Physiol Rev 2018;98:3-58.
47. Kugiyama K, Ohgushi M, Motoyama T, Hirashima O, Soejima H, Misumi K, et al. Intracoronary infusion of reduced glutathione improves endothelial vasomotor response to acetylcholine in human coronary circulation. Circulation 1998;97:2299-2301.
48. Knolle PA, Wohlleber D. Immunological functions of liver sinusoidal endothelial cells. Cell Mol Immunol 2016;13:347-353.
49. Pober JS, Merola J, Liu R, Manes TD. Antigen Presentation by Vascular Cells. Front Immunol 2017;8:1907.

50. Wang J, Hu W, Shen Z, Liu T, Dai W, Shen B, et al. Dissecting the single-cell transcriptomeunderlying chronic liver injury. Mol Ther Nucleic Acids 2021;26:1364-1373.
51. Chaparro M, Sanz-Cameno P, Trapero-Marugan M, Garcia-Buey L, Moreno-Otero R. Mechanisms of angiogenesis in chronic inflammatory liver disease. Ann Hepatol 2007;6:208-213.
52. Friedrich T, Ferrante F, Pioger L, Nist A, Stiewe T, Andrau JC, et al. Notch-dependent and -independent functions of transcription factor RBPJ. Nucleic Acids Res 2022;50:7925-7937.
53. Karki A, Mantyla E, Hirsimaki Y, Karlsson S, Toikkanen S, Hirsimaki P. Comparison of the effects of tamoxifen and toremifene on rat hepatocarcinogenesis. Arch Toxicol 2000;74:249-256.
54. Kohigashi K, Fukuda Y, Imura H. Inhibitory effect of tamoxifen on diethylstilbestrol-promoted hepatic tumorigenesis in male rats and its possible mechanism of action. Jpn J Cancer Res 1988;79:1335-1339.

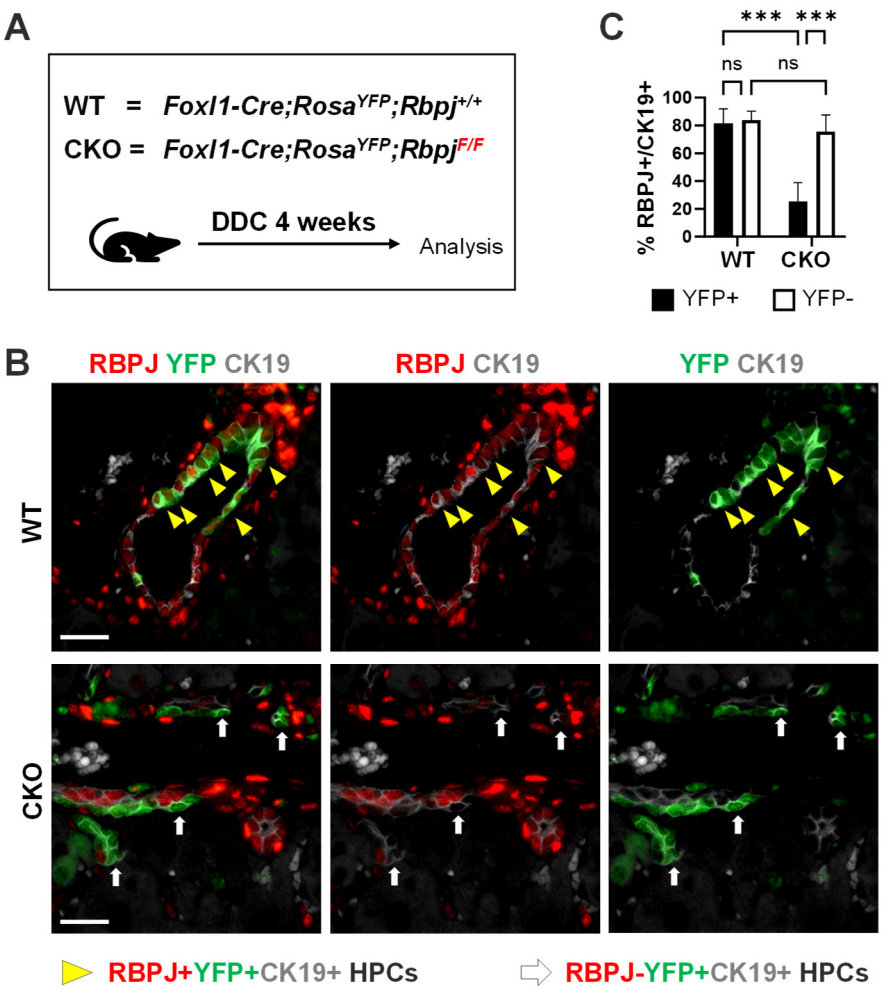

Figure 1. Conditional deletion of *Rbpj* in HPCs using *Foxl1-Cre*. (A) Schematic representation of the experimental strategy. 10- to 11-week-old male mice were treated with the DDC diet for 4 weeks. (B) Immunofluorescence analysis. Top panels: RBPJ protein is expressed in YFP+CK19+ HPCs (yellow arrowheads) and surrounding mesenchymal cells in portal areas of WT livers. Bottom panels: RBPJ protein expression is lost specifically in HPCs (white arrows) of CKO livers. Scale bar, 25 μm. (C) Quantification of the percentage of RBPJ-expressing cells within the CK19+ biliary population. Data are expressed as mean ± standard deviation; n = 3-4 mice per group; *** $p < 0.001$; ns, not significant. Abbreviations: CK19, cytokeratin 19; CKO, conditional knockout; DDC, 3,5-diethoxycarbonyl-1,4-dihydrocollidine; HPC, hepatic progenitor cell; RBPJ: recombination signal binding protein for immunoglobulin kappa J region; WT, wild-type; YFP, yellow fluorescent protein.

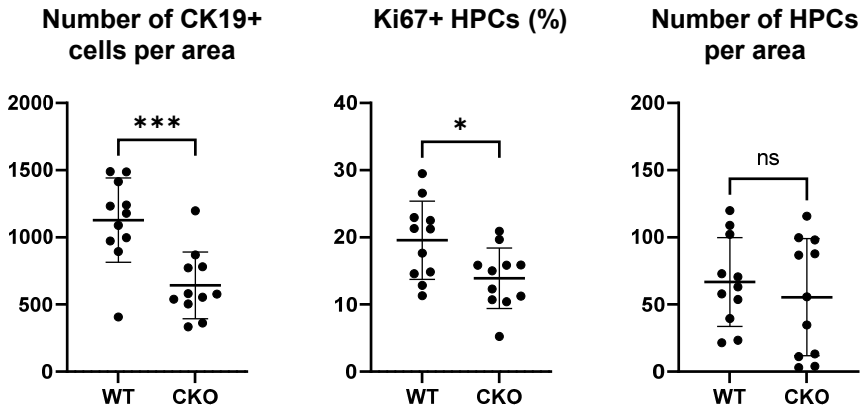

Figure 2. Ductular reactions and proliferation of HPCs are attenuated in CKO mice. Following immunofluorescence staining of liver sections, portal areas were captured and subjected to quantitative analysis of cell numbers. (A) Number of CK19+ cells per area. (B) Percentage of Ki67+ HPCs in relation to the total number of HPCs. (C) Number of HPCs per area. All data are expressed as mean ± standard deviation; n = 11 mice per group; * $p < 0.05$; *** $p < 0.001$; ns, not significant. Abbreviations: CKO, conditional knockout; CK19, cytokeratin 19; HPC, hepatic progenitor cell; WT, wild-type.

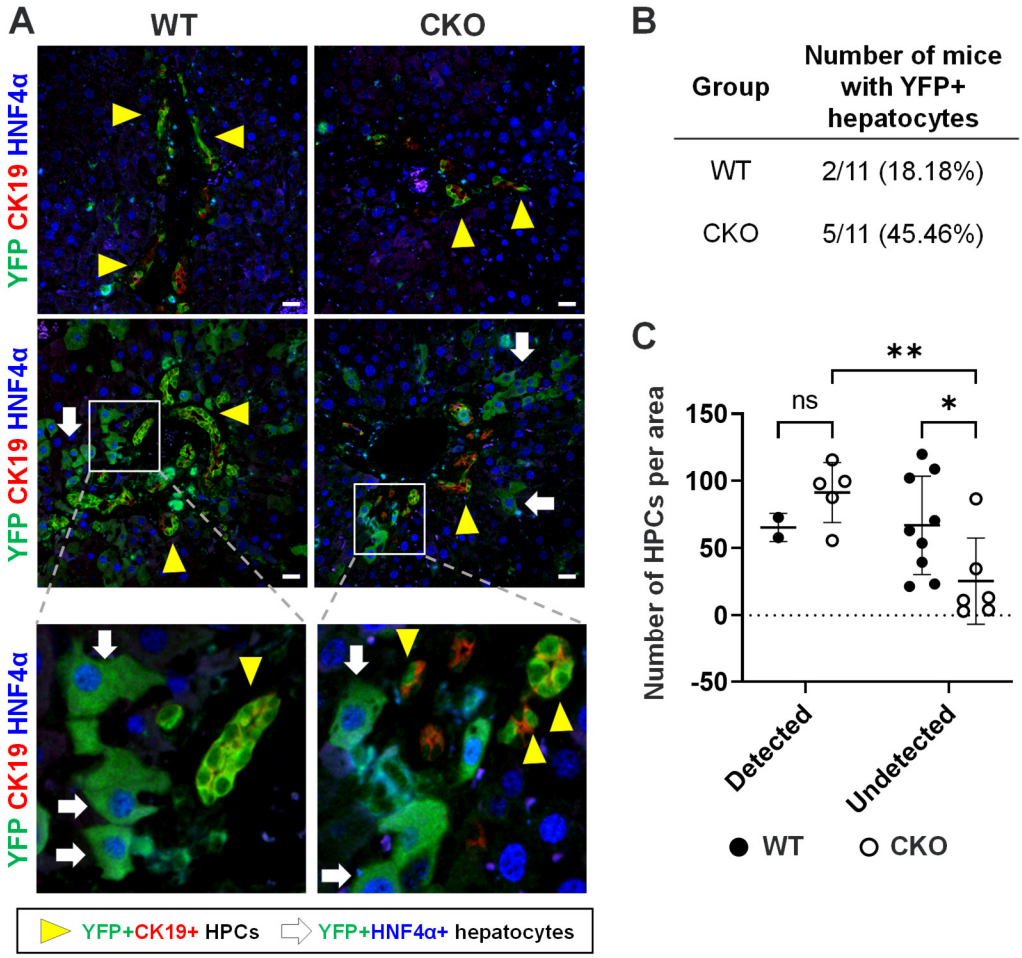

Figure 3. The percentage of mice in which lineage-labeled hepatocytes are detected is increased in response to *Rbpj* deletion. (A) Immunofluorescence analysis. Yellow arrowheads, YFP+CK19+ HPCs. White arrows, YFP+HNF4α+ hepatocytes. Top panels: Representative images of WT and CKO livers without YFP+HNF4α+ hepatocytes. Middle and bottom panels: Representative images of WT and CKO livers in which YFP+HNF4α+ hepatocytes are detected. Scale bar, 25 μm. (B) The number and percentage of mice in which YFP+ hepatocytes are detected. (C) The number of HPCs per area is high in CKO mice in which YFP+ hepatocytes are detected (Detected) as compared to CKO mice devoid of YFP+ hepatocytes (Undetected). The number of HPCs per area is reduced in CKO mice compared to WT mice only in the undetected group. Data are expressed as mean ± standard deviation. A total of 11 mice per genotype were analyzed separately (n = 2-9 per group) based on the presence of YFP+ hepatocytes; * $p < 0.05$; ** $p < 0.01$; ns,

not significant. Abbreviations: CK19, cytokeratin 19; CKO, conditional knockout; HNF4α, hepatocyte nuclear factor 4 alpha; HPC, hepatic progenitor cell; RBPJ, recombination signal binding protein for immunoglobulin kappa J region; WT, wild-type; YFP, yellow fluorescent protein.

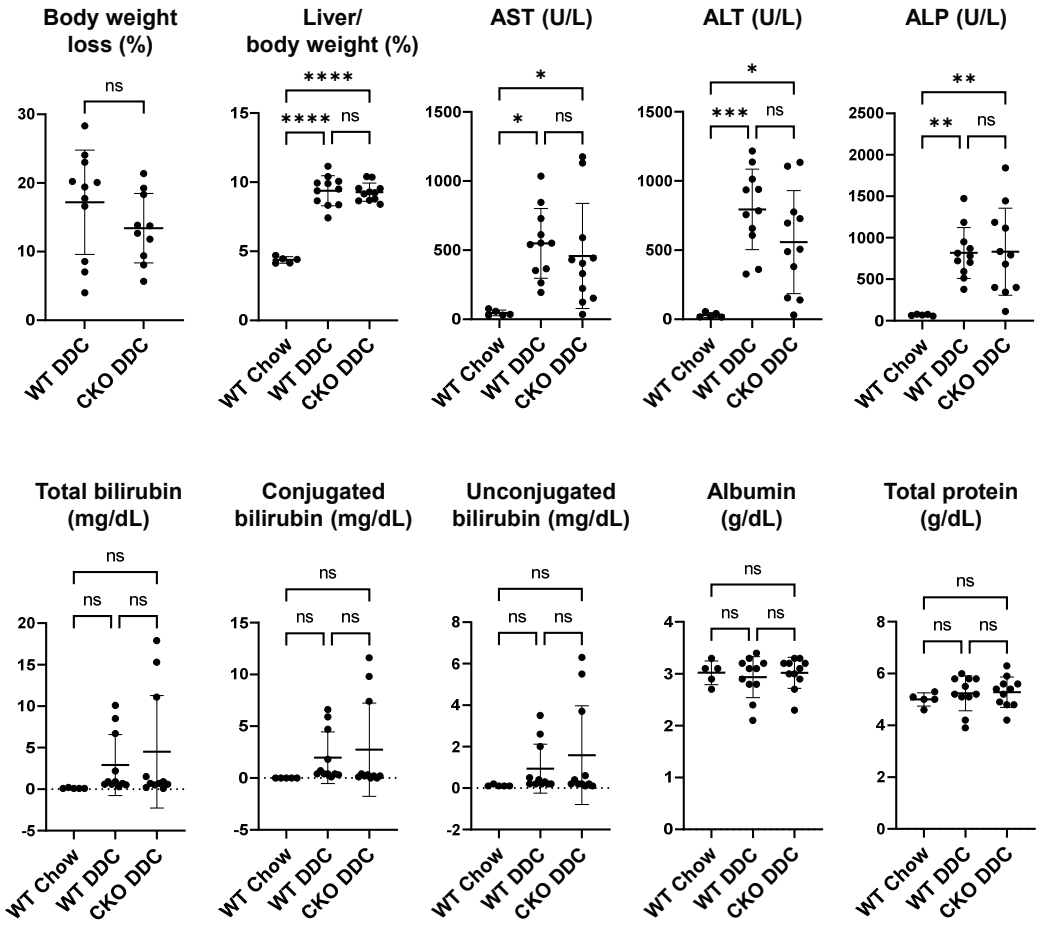

Figure 4. Serum markers of liver injury and function. All data are expressed as mean ± standard deviation; n = 5-11 mice per group. Abbreviations: ALP, alkaline phosphatase; ALT, alanine aminotransferase; AST, aspartate aminotransferase. * $p < 0.05$; ** $p < 0.01$; *** $p < 0.001$; **** $p < 0.0001$; ns, not significant.

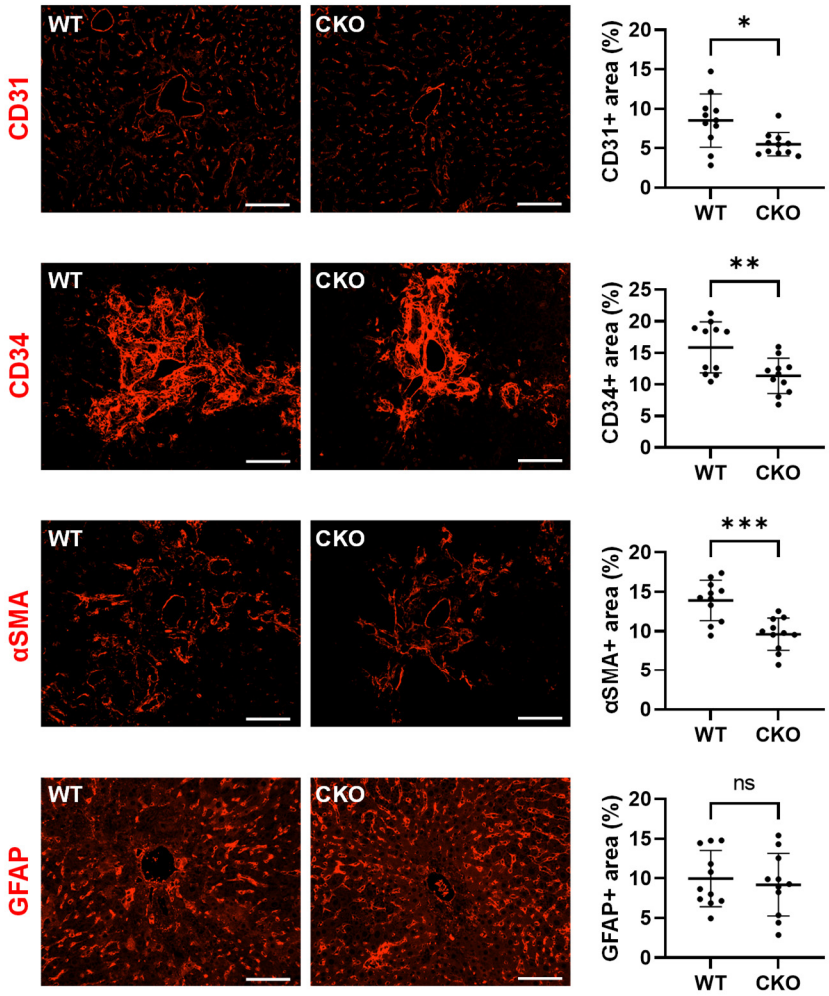

Figure 5. Endothelial and fibrotic marker-positive areas are reduced in CKO mice compared to WT mice. Left panels: Immunofluorescence analysis of portal areas. Scale bar, 100 μm. Right panels: Quantification of marker-positive areas. All data are expressed as mean ± standard deviation; n = 11 mice per group. * $p < 0.05$; ** $p < 0.01$; *** $p < 0.001$; ns, not significant. Abbreviations: αSMA, alpha smooth muscle actin; CKO, conditional knockout; GFAP, glial fibrillary acidic protein; WT, wild-type.

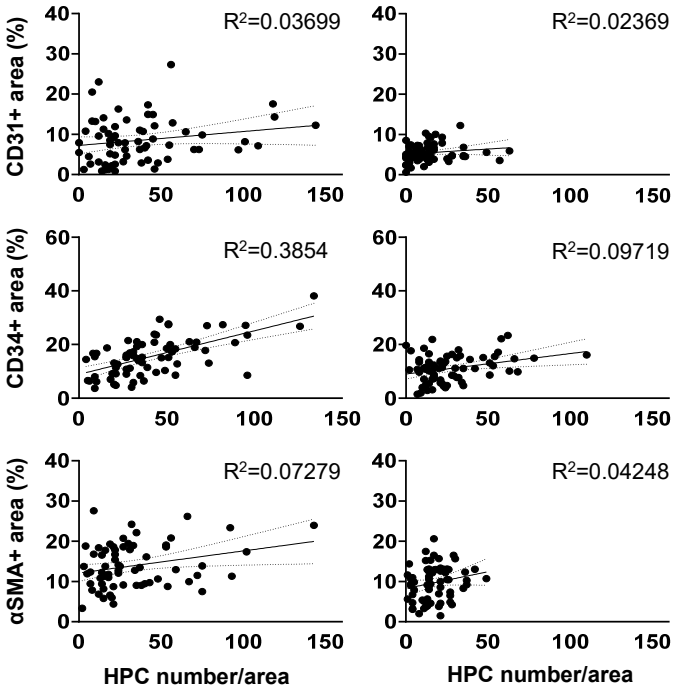

Figure 6. HPC-specific *Rbpj* knockout attenuates correlations between the areas positive for CD31, CD34, and αSMA and the number of HPCs. Each dot represents one captured area in which marker-positive cells and HPCs are detected (n = 66-72 per group). R^2, square of the correlation coefficient. Abbreviations: αSMA, alpha smooth muscle actin; HPC, hepatic progenitor cell.

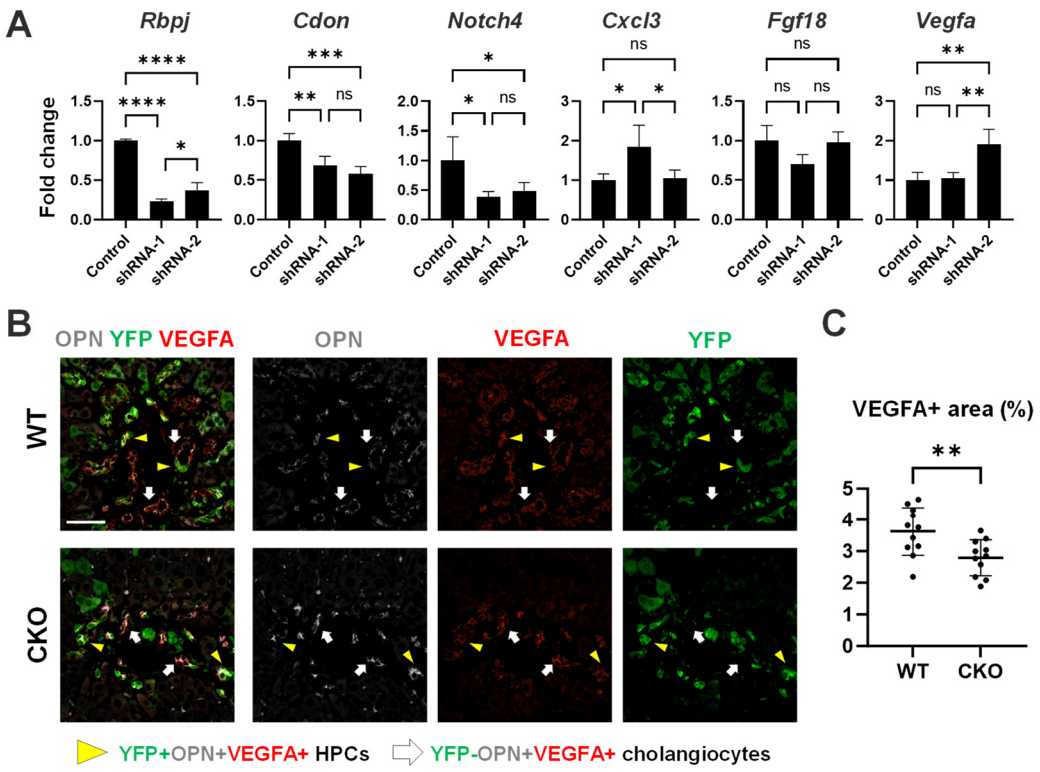

Figure 7. VEGFA-positive area is reduced in CKO compared to WT. (A) qPCR analysis was performed using HPCs transduced with lentiviral vectors expressing two different shRNAs against *Rbpj* (shRNA-1 and shRNA-2) and a non-silencing control and then subjected to puromycin selection. Data are expressed as mean ± standard deviation; n = 4 independent experiments. (B) Immunofluorescence analysis. Yellow arrowheads, YFP+OPN+VEGFA+ HPCs. White arrows, YFP-OPN+VEGFA+ cholangiocytes. Scale bar, 50 µm. (C) Quantification of VEGFA+ areas. Data are expressed as mean ± standard deviation; n = 11 mice per group. * $p < 0.05$; ** $p < 0.01$; *** $p < 0.001$; **** $p < 0.0001$; ns, not significant. Abbreviations: CKO, conditional knockout; HPC, hepatic progenitor cell; OPN, osteopontin; qPCR, quantitative polymerase chain reaction; VEGFA, vascular endothelial growth factor A; WT, wild-type; YFP, yellow fluorescent protein.

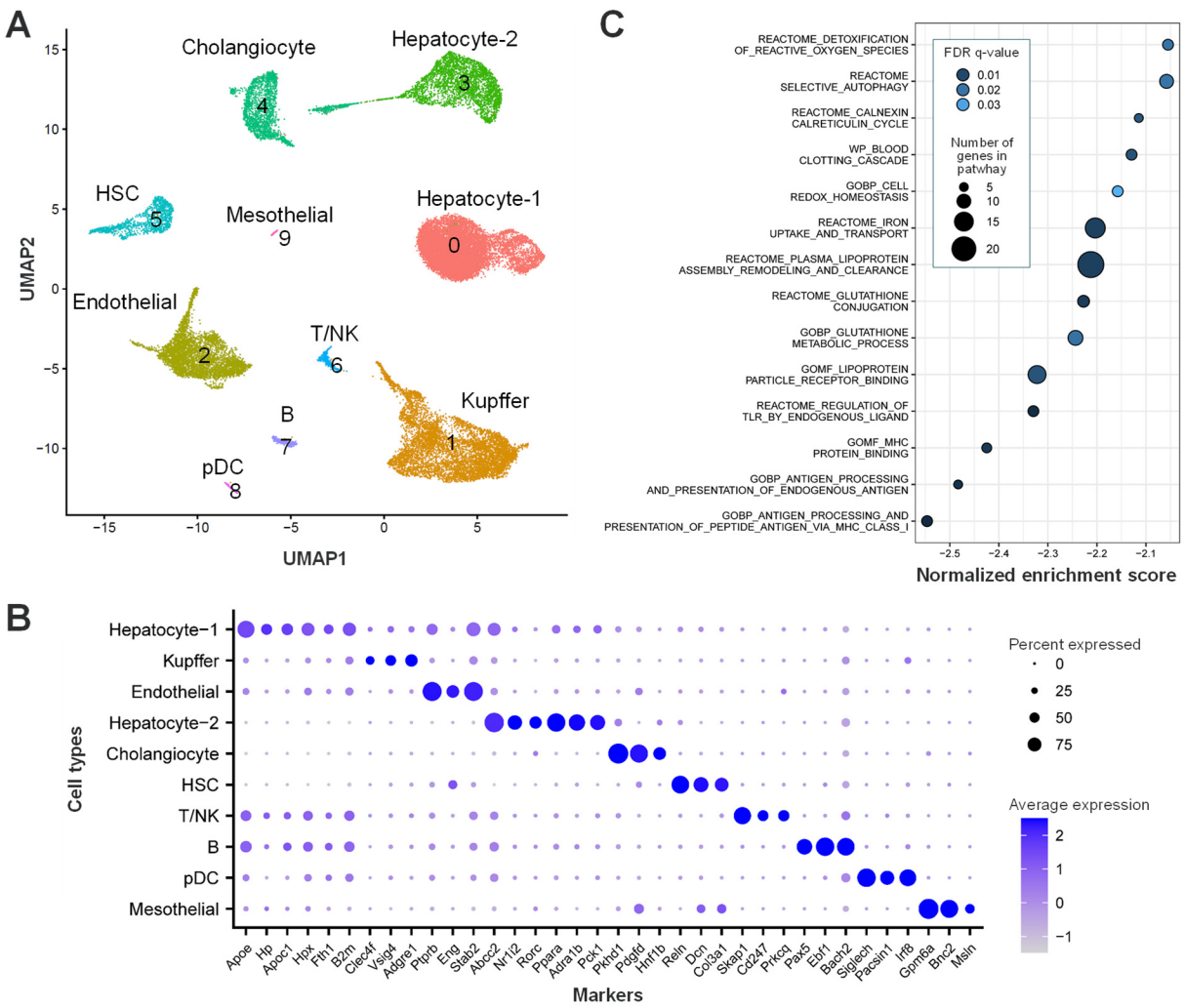

Figure 8. sNuc-seq reveals the impact of conditional HPC modulation on endothelial gene expression. (A) UMAP plot showing 10 clusters. (B) Representative markers of each cluster. Genes associated with distinct metabolic processes are shown for hepatocyte clusters; GOCC_HIGH_DENSITY_LIPOPROTEIN_PARTICLE (*Apoe, Hp, Apoc1*), GOBP_IRON_ION_HOMEOSTASIS (*Hpx, Fth1, B2m*), GOBP_XENOBIOTIC_METABOLIC_PROCESS (*Abcc2, Nr1i2, Rorc*), GOBP_GLUCOSE_METABOLIC_PROCESS (*Ppara, Adra1b, Pck1*). (C) GSEA was performed using Cluster 2 genes downregulated in CKO compared to WT and selected enriched terms were shown. An FDR q-value of <0.25 was considered statistically significant in this study. Abbreviations: CKO, conditional knockout; FDR, false discovery rate; GSEA, gene set enrichment analysis; HPC, hepatic progenitor cell; HSC, hepatic

stellate cell; NK, natural killer; pDC, plasmacytoid dendritic cell; sNuc-seq, single-nucleus RNA sequencing; UMAP: uniform manifold approximation and projection; WT, wild-type.